

Article

A Precipitation-Based Process to Generate a Solid Formulation of a Therapeutic Monoclonal Antibody: An Alternative to Lyophilization

Athanas A. Koynov , Wei Lin , Jameson R. Bothe, Luke Schenck , Bibek Parajuli, Zhao Li , Richard Ruzanski , Natalie Hoffman, Derek Frank and Zachary VanAernum

Merck & Co., Inc., Rahway, NJ 07065, USA

* Correspondence: athanas.koynov@merck.com (A.A.K.); wei.lin3@merck.com (W.L.)

Abstract: Lyophilization, or freeze-drying, is the default technique for the manufacture of solid-state formulations of therapeutic proteins. This established method offers several advantages, including improved product stability by minimizing chemical degradation, reduced storage requirements through water removal, and elimination of cold chain dependence. However, the lyophilization process itself presents limitations. It is a lengthy, batch-based operation, potentially leading to product inconsistencies and high manufacturing costs. Additionally, some proteins are susceptible to structural alterations during the freezing step, impacting their biological activity. This paper presents an alternative approach based on the co-precipitation of protein and excipients using an organic solvent. We explore the impact of various processing parameters on the viability of the formulation. We also provide an extensive characterization of proteins reconstituted from precipitated formulations and compare protein stability in solution and in lyophilized and precipitated solid formulations under long-term, accelerated, and stressed storage conditions.

Keywords: precipitation; solid formulation; lyophilization; protein characterization; protein stability; co-processed API



Academic Editor: Fernando Albericio

Received: 25 November 2024

Revised: 27 January 2025

Accepted: 28 January 2025

Published: 31 January 2025

Citation: Koynov, A.A.; Lin, W.; Bothe, J.R.; Schenck, L.; Parajuli, B.; Li, Z.; Ruzanski, R.; Hoffman, N.; Frank, D.; VanAernum, Z. A

Precipitation-Based Process to Generate a Solid Formulation of a Therapeutic Monoclonal Antibody: An Alternative to Lyophilization. *J. Pharm. BioTech Ind.* **2025**, *2*, 2. <https://doi.org/10.3390/jpbi2010002>

Copyright: © 2025 by the authors. Licensee MDPI, Basel, Switzerland. This article is an open access article distributed under the terms and conditions of the Creative Commons Attribution (CC BY) license (<https://creativecommons.org/licenses/by/4.0/>).

1. Introduction

In recent years, biologics have represented an ever-increasing share of new FDA approvals (compared to small molecules), surpassing 50% for the first time in 2022 [1]. This increase translates into a proportionally increased demand for commercial sterile lyophilization capacity as close to half of all therapeutic protein products are formulated in the solid state [2]. While stability is the primary driver for the development of solid formulations in the biologics product space, worldwide distribution logistics and patient compliance present important considerations. With an expected growth in biosimilar and antibody–drug conjugate filings in the next few years, the demand for lyophilization capacity will only increase further, potentially surpassing current supply levels.

While lyophilization is the de facto technology for the manufacture of solid, room-temperature-stable formulations of large molecules, there are several technical issues driving the search for alternative drying methods. Lyophilization, as a process, is time and capital-intensive [3,4]. There are also potential issues associated with stability (e.g., damage due to freeze concentration, freezing stresses from the formation of dendritic crystals, etc.) [5,6] and lyophilized cake physical properties control [7], as well as potential risks around sequential batch cross-contamination, residual moisture control, etc. [8].

The main alternatives to lyophilization include methods based on solvent evaporation rather than sublimation, which has some limitations. Spray-drying [9,10] is a process where the solution of the biomolecule and excipients is atomized into droplets through a nozzle and sprayed into a drying chamber. There are technical risks associated with spray-drying, which are mostly due to the potential for damage to the biomolecule [11] due to thermal stresses caused by the higher drying temperatures, interfacial stresses at the surfaces of the sprayed droplets, and shear forces in the nozzle [12–16], as well as compositional gradients in the isolated solids [17] due to disparate kinetics of diffusion of the various excipients. However, the main hurdle, which has precluded the widespread use of spray-drying with biologics, is that of sterile implementation, which typically limits applicability to, e.g., formulations for inhalation delivery [18–21].

Other examples of evaporative drying include Foam Vacuum Drying [10] as well as microwave-assisted Vacuum Drying [22,23]. Both of these processes reduce the drying times and some freeze-associated risks, but at greatly increased operating costs.

A side-by-side comparison of the performance of three different drying processes (lyophilization, spray-drying, and foam drying) for the formulation of a live attenuated influenza vaccine is presented in [24]. The authors arrive at the conclusion that the drying process can have a significant impact on the stability of the final product (even after individual process optimizations).

In this context, this work considers a bulk precipitative approach rather than an evaporative one for water removal and the subsequent isolation of solid-state formulations of biologics. Precipitative approaches offer multiple attractive attributes: they exhibit typically unlimited scalability and throughput, can be implemented in standard reactors, eliminating the need for costly processing solutions, and, most importantly, replace the terminal drying of water with that of a volatile organic solvent. Potential drawbacks include the need for added aseptic processing controls compared to water removal *in situ* in the product vials, as well as the ability to process using organic solvents, which is an uncommon feature in most biologics manufacturing sites. The implementation of a sterile process based on this approach, while challenging, would be less complicated than in the case of spray-drying, mostly due to the fact that aseptic filtration and drying of the precipitated slurry can be accomplished entirely using vacuum techniques.

Protein precipitation in organic solvents is a well-established technique [25]. It is commonly used for protein purification and concentration [26–28] in, e.g., sample preparation for proteomic analysis. It has substantial advantages compared to other methods involving extraction and buffer exchange through dialysis, in addition to speed and convenience in lyophilization and re-solubilization. There are substantial risks as well, stemming from the potential for protein aggregation caused by denaturation leading to difficulties in re-solubilizing the solid precipitate.

A proprietary technique called Microglassification™ [29] implements a similar process, where the water from droplets of a protein solution is extracted into a secondary “dehydrating” solvent, yielding spherical beads of glassified protein. The advantages of this process include the ability to produce excipient-free solid protein products, as well as the precise control of the physical characteristics of the resulting particles. Its disadvantages involve scalability and cost [30,31].

In the typical protein precipitation process, as organic solvent is added to the system, the folding of the protein changes due to preferential interactions between the solvent and hydrophobic and aromatic residues. At intermediate solvent contents, as a consequence of these interactions, proteins tend to form a gel phase. As the solvent content increases further, the protein unfolding is increased, accompanied by a loss of hydration, leading to the eventual precipitation [32].

While serving a different goal, precipitation is also one of the earliest methods used for large-scale protein purification and is still used for the purification of plasma proteins [33]. The precipitation process involves the use of ethanol, salt, pH, and temperature to control the selectivity of protein precipitation. Recent developments have shown increased interest in the use of precipitation for the initial purification (capture) of monoclonal antibody (mAb) products. This is attributed to the significant increase in product titer and lower cost compared with traditional column chromatography methods [34,35]. Additional precipitants have been investigated for mAb precipitation, including calcium chloride (CaCl₂) [36], zinc chloride (ZnCl₂) and PEG [37], and elastin-like polypeptides (ELPs) among others [38,39].

Additionally, precipitative approaches have seen extensive application in the removal of impurities such as host cell proteins (HCPs) and DNA. Precipitation aides have included calcium chloride [40,41], caprylic acid [42], and cationic polymers [43], e.g., polyallylamine (PAA), partially benzylated polyallylamine, polyarginine, pDADMAC, and polyethyleneimine (PEI) [43–47].

While precipitative techniques have been used for the successful precipitation of pure protein, long-term storage stability, a prerequisite for any successful formulation, necessitates the inclusion of stabilizing excipients.

The most commonly used protein stabilizers are sugars and polyols. There are two competing hypotheses aiming to explain the mechanism of this stabilization: vitrification and water replacement [48,49]. According to the vitrification hypothesis, stabilization occurs by virtue of the enclosure of the protein in a rigid glassy amorphous matrix composed of sugar molecules. This matrix conformationally confines the protein, preventing the unfolding and diffusion necessary for aggregation. The water replacement theory, on the other hand, postulates that, as the hydration layer is disrupted during the removal of the water (in this case by replacement with organic solvent), the hydroxyl groups on the sugar molecules take the place of the water, forming hydrogen bonds with the protein. This hydrogen bonding substitution allows the protein to maintain its native folded state [50,51]. Recent publications suggest that the two hypotheses can be reduced to a common mechanism [52].

Regardless of which theory holds true, in either case, there would be a kinetic component to the formation of the stabilizing structure. For vitrification to be successful, the glassy matrix must form on time scales shorter than those associated with protein unfolding in the presence of the organic solvent, and its subsequent diffusion and potential aggregation. Similarly, in water replacement, there is a kinetic rate associated with the substitution of the water with sugar molecules in hydrogen bonding to the protein. Since in both cases, the precipitation kinetics have the potential to affect the effectiveness of the stabilization mechanism, the process can be optimized to maximize product stability.

Multiple parameters can affect the kinetics of precipitation, including protein concentration, organic solvent type and solvent/anti-solvent ratio, temperature, and solvent addition rate.

Protein degradation pathways in the solid state fall into two broad categories, physical and chemical, with the former comprising mostly denaturation and non-covalent aggregation, and the latter consisting of covalent aggregation, deamidation, and oxidation [48].

The purpose of this work is to demonstrate the feasibility of a precipitative approach to produce solid-state formulations of biologics as an alternative to lyophilization. This is a conceptual, proof-of-concept work, as, in addition to the actual precipitative process, a commercial-scale implementation for a therapeutic product would also need to overcome additional hurdles, such as, e.g., maintaining sterility during the filtration, drying, and discharging of the solid precipitate in the filter-dryer. Additional logistical issues would

include the storage and transportation of the bulk powder under sterile conditions as well as the filling of vials.

Another consideration would be the control of residual solvents in the solids after drying in accordance with, e.g., ICH Q3C. Since the mechanism of the precipitative process likely involves the formation of complexes between the solvent and hydrophobic and aromatic residues on the protein, the removal of residual solvent during drying would have to overcome the energetic barrier associated with these complexes.

Here, we apply a precipitation approach to a monoclonal antibody, which is known to have poor chemical stability in the liquid state where a succinimide intermediate is known to form in the complimentary determining region, reducing potency [53].

A typical lyophilized formulation needs to meet certain requirements, specifically, it needs to stabilize the cake against collapse during drying, as well as limit the use of excipients with a high vapor pressure under the drying conditions, to limit the risk of sublimation. While the optimal excipient composition of a precipitated solid formulation would likely differ from one optimized for lyophilization (and in fact, the upside of precipitation may be a wider selection of excipients, given that cake collapse and excipient sublimation are not constraints), in this work, the authors have kept the formulation between lyophilization and precipitation identical (the exact formulation composition is not included in this work). On one hand, this limits the power of the precipitative process, potentially allowing a loss of product stability, which could have been mitigated through excipient optimization. On the other hand, it removes the potential impact of excipient composition differences on the properties of the freeze-dried and precipitated formulations compared in this work.

2. Materials and Methods

2.1. Monoclonal Antibody

Monoclonal antibody, (mAb) X, an IgG4 molecule with a pI of around 7.0, was used in this study. The starting material for this study is the formulated drug substance (DS), where typical bulking agents and surfactants for stabilizing mAb formulation during long-term storage have been added. The bulk DS was received frozen at $-80\text{ }^{\circ}\text{C}$, and materials were thawed freshly when needed. The DS used in precipitation experiments was from the same bulk material so the starting concentrations and quality attributes were the same. The drug substance after freeze–thaw was filtered through $0.2\text{ }\mu\text{m}$ polyethersulfone membranes (MilliporeSigma, Merck KGaA, Darmstadt, Germany) to remove any aggregated/undissolved protein prior to use.

2.2. Precipitation Process

The mAb solution (DS) was added to the organic solvent (in reverse addition), using a Henke Sass Wolf GmbH 3 mL syringe fitted with a 20 Ga 1.5'' tipless needle, under different conditions. The precipitated slurry was filtered using a $0.45\text{ }\mu\text{m}$ Whatman[®] Autovials[™] PVDF membrane syringeless filter (Cytiva, Marlborough, MA, USA). A follow-up displacement wash of acetone was filtered through the wet cake. The washed cake was dried in the filter using a vacuum pulled from the bottom and a light nitrogen sweep from the top for 12 h, at which time the dry cake was transferred to a 20 mL scintillation vial (borosilicate glass vial with a polypropylene cap) and stored at $2\text{--}8\text{ }^{\circ}\text{C}$.

Preliminary experiments assessing the feasibility of several solvents considered acetone, as well as methyl, ethyl, and isopropyl alcohol, at different temperatures. Of these, only acetone yielded well-behaved solid particles after isolation. Particles precipitated in acetone did not tend to agglomerate, filtered well (the liquors from the precipitation would filter through the wet cake in under a minute), and upon drying, the dry cake easily

dispersed into individual particles. Precipitation in alcohols resulted in either gelling or very soft particles that fouled the filter.

Once acetone was selected as the precipitation solvent, an initial set of precipitations was performed to assess the reproducibility of the process. Three identical precipitations were carried out into cold acetone ($-20\text{ }^{\circ}\text{C}$) at a 100 mL scale, with agitation provided by magnetic stir bars at 300 rpm. A typical precipitated powder is shown in Figure 1. These three batches were pooled and staged under stability conditions at $5\text{ }^{\circ}\text{C} \pm 3\text{ }^{\circ}\text{C}$ and $25\text{ }^{\circ}\text{C} \pm 2\text{ }^{\circ}\text{C}$ with 60% relative humidity, and $40\text{ }^{\circ}\text{C} \pm 2\text{ }^{\circ}\text{C}$ with 75% relative humidity for 3 months. The stability profile was compared to those of the liquid formulation (stability at $5\text{ }^{\circ}\text{C} \pm 3\text{ }^{\circ}\text{C}$ and $25\text{ }^{\circ}\text{C} \pm 2\text{ }^{\circ}\text{C}$ with 60% relative humidity) and lyophilization (same stability conditions).

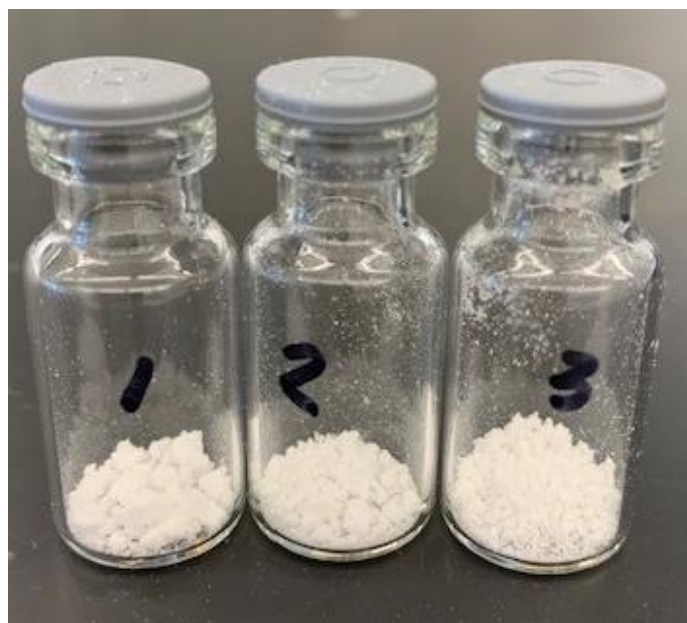


Figure 1. Typical precipitated powders correspond to the three repeat runs for the experimental conditions 1'.

Process characterization was carried out by varying operating parameters to assess the impact of the kinetics of precipitation, as influenced by solvent temperature, mixing intensity, and anti-solvent volume. Not all parameter combinations were completed, but experiments were run with parameter combinations representing the highest and lowest thermal and shear stresses. For the cases of no mixing and medium mixing, the solvent was added to a 20 mL scintillation vial. In the “no mixing” experiments, the mAb solution was charged to the quiescent solvent. In the medium mixing experiments, the scintillation vial was placed on an IKA RCT stir plate and the solvent was agitated using a ChemGlass PTFE magnetic stir bar (CG-2001-01) (at 300 rpm). The high mixing experiments were carried out using an IKA ULTRA-TURRAX[®] homogenizer Tube Drive (Staufen, Germany), with the solvent added to a DT-20 20 mL tube, and the drive engaged at 3000 rpm.

In all cases, 1 mL of the mAb solution was charged to the solvent above the surface over ~ 3 s. The volume of organic solvent in all experiments was $10\times$ that of the solution (or 10 mL), except for the two experiments denoted with an asterisk in the table below, where the volume of the solvent was $3\times$ (or 3 mL). Also, in all cases, the temperature of the follow-up acetone wash matched the precipitation temperature. Following these, nine additional precipitations were carried out at the conditions outlined in Table 1.

Table 1. Precipitation process conditions evaluated in the experiments.

Sample Number	Solvent Temperature	Mixing
1'	−20 °C	Medium
1	25 °C	None
1*	25 °C	None
2	25 °C	High
3	0 °C	None
4	0 °C	High
5	−20 °C	High
5*	−20 °C	High
6	0 °C	Medium
7	25 °C	Medium

* A different solvent to anti-solvent volume ratio was used (3×); 1' corresponds to the conditions of the initial triplicate run.

2.3. Analytical Characterization

2.3.1. Critical Quality Attributes

The dry solid material was reconstituted using Milli-Q ultrapure water (Millipore-Sigma, Burlington, MA, USA) prior to protein concentration determination by Slope Spectroscopy (SoloVPE, Repligen, Waltham, MA, USA).

Charge variant analysis was performed using an Alliance HPLC (Waters Corporation, Milford, MA, USA) equipped with a dual absorbance detector set at 280 nm. The samples were diluted to 8 mg/mL with purified water and about 80 µg was loaded into a ProPac SCX-10 BioLC Analytical column (4 × 250 mm, Thermo Fisher Scientific, Waltham, MA, USA). The main, acidic, and basic peaks of the samples were separated and reported as a percent of the relative peak area.

Size variant analysis via size exclusion chromatography (SEC) was performed using an Acquity UPLC (Waters Corporation, Milford, MA, USA) equipped with a UV detector set at 280 nm. The samples were diluted to 5 mg/mL with the mobile phase and about 30 µg was loaded into an Acquity BEH200 SEC column (4.6 × 300 mm, Waters Corporation). The monomer and high molecular weight (HMW) species were separated and reported as percent relative peak area.

Total impurities and the level of low molecular weight (LMW) species were determined using reduced and non-reduced CE-SDS, respectively. The CE-SDS analyses were performed using a ProteomeLab PA800 Plus (Sciex, Farmingham, MA, USA) equipped with a PDA detector set at 220 nm and a pre-assembled capillary cartridge. The samples were diluted to 10 mg/mL with purified water and either reduced in an SDS buffer containing 2-mercaptoethanol (reduced conditions) or denatured in an SDS buffer containing N-ethylmaleimide (non-reduced conditions) at 70 °C for 10 min prior to separation in CE-SDS analyses.

2.3.2. Biological Characterization

As part of the analytical characterization of the mAb, the potency of the material was assessed in an enzymatic assay where mAb binding inhibits enzymatic activity, which is measured by the conversion of a fluorescent substrate. IC₅₀ values, the concentration of mAb reference material, and test samples that exhibit 50% of the maximal inhibition were determined using a four-parameter logistic curve fitting analysis. Relative potency was calculated by applying a Parallel Line Analysis of dose–response curves using appropriate statistical software.

2.3.3. Biophysical Characterization

Fluorescence Spectroscopy: Fluorescence Spectroscopy was performed on protein solutions at 0.5 mg/mL concentration using Horiba Fluoromax-4. Tryptophan was selec-

tively excited using the excitation wavelength of 295 nm with an emission range set at 300–550 nm. Instrumental conditions were as follows: total accumulations of 3 (averaged), both excitation and emission slit widths were set at 2.0 nm, and the sample temperature was set at 20 °C. Diluent spectra were measured prior to the test sample as a reference. The net fluorescence of the test sample was subtracted against the diluent and was normalized against its concentration and wavelength for maximal intensity (λ_{max}), which was determined based on net fluorescence intensity.

Circular Dichroism (CD): CD was used for secondary and tertiary structure determination. CD was measured on a JASCO J-1500 CD Spectropolarimeter equipped with a temperature control system (JASCO International, Tokyo, Japan). The instrument detector chamber was purged with nitrogen gas for at least 5 min before sample measurement.

Far UV CD was used for secondary structure determination. Samples at 1 mg/mL were prepared in aqueous solution. Spectra were obtained in a 0.01 cm quartz cylindrical cell (Hellma Analytics, Müllheim, Germany) at 20 °C. Instrument conditions were as follows: data pitch of 0.2 nm, bandwidth of 1 nm, scanning speed at 50 nm/min, response time of 4 s, and scanning wavelength range within 190–280 nm with continuous scanning mode. The spectra recorded were the average of five accumulated scans. The diluent spectrum was collected prior to the test sample as a reference. Collected data were normalized by concentration, path length, and number of amino acids in the molecule and reported as mean residual ellipticity. Background diluent was subtracted from the sample spectra. Raw data were exported from JASCO as .csv files and data were deconvoluted using custom model fit spectra over a wavelength range of 190–280 nm using CDNN software (Version 2.1) to assess overall alpha helix and beta sheet content.

Near UV CD was used for tertiary structure determination. Samples at 1 mg/mL were prepared in aqueous solution. Spectra were obtained in a 1 cm quartz cuvette (Hellma Analytics) at 20 °C. Instrument conditions were as follows: data pitch 0.2 nm, bandwidth 1 nm, scanning speed 50 nm/min, response time 2 s, and scanning wavelength within 240–350 nm with continuous scanning mode. The spectra recorded were the average of five accumulated scans. The diluent spectrum was collected prior to the test sample as a reference. Collected data were normalized by concentration, path length, and number of amino acids in the molecule and reported as mean residual ellipticity. Background diluent was subtracted from the sample spectra. Raw data were exported from JASCO as .csv files and all datasets were plotted using GraphPad Prism 9.

Differential Scanning Calorimetry: The thermal stability of protein was determined using Differential Scanning Calorimetry on Microcal PEAQ DSC (Malvern Instruments, Worcestershire, UK). Samples at 1 mg/mL concentration were prepared in sample diluent. The heating rate was set at 1.5 °C/min in the temperature ranges between 15 and 95 °C. Duplicate measurements were performed for each sample. The thermogram of the respective buffer was subtracted from the sample thermogram. A baseline subtraction was performed to obtain DSC thermograms, adjusting the baseline to zero.

Dynamic Light Scattering (DLS): Overall size distribution and higher-order structure were determined using Dynamic Light Scattering. For DLS measurement, samples were first diluted to 10 mg/mL concentrations using relevant diluent placebo and allowed to equilibrate (2 min). Hydrodynamic size distribution was measured at 20 °C using a Malvern Lamp One Source with 10 repetitions for each run. Triplicate run measurements were averaged in Zetasizer software (Version 7.13) to obtain the reported results.

3. Results and Discussion

3.1. Process Reproducibility and Formulation Characterization

A comprehensive set of analytical assays was utilized to assess the impact of the precipitation process parameters on the quality of mAb X.

Figure 2 shows the comparative results from the characterization of reconstituted solutions from the three identical precipitation batches described above and the mAb prior to precipitation. Protein concentration measurements demonstrated that the levels of mAb X (% *w/w*) in all three precipitation batches were very similar as well as comparable to the target level in the pre-precipitation material. Selected quality attributes, including charge and size variants, were analyzed using CEX, SEC, and CE-SDS. The levels of acidic and basic variants for the triplicate precipitations were very similar before and after precipitation, with 18.3–18.5% and 29.7–30.0%, respectively. The levels of total HMW species, LMW species, and total impurities were also comparable, with 1.2–1.7%, 1.9–2.0%, and 1.3–1.4%, respectively. Product attributes were consistent among the three lots, demonstrating the reproducibility of the precipitation process. Moreover, the levels of charge variants, size variants, and impurities of the three lots were comparable to those of the pre-precipitation material, indicating that the product quality of the mAb was maintained during the precipitation process.

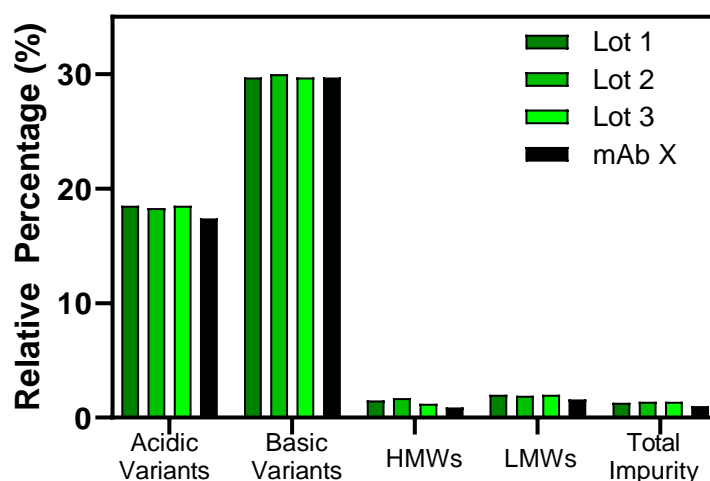


Figure 2. Reproducibility of the precipitation process: a comparison of critical quality attributes of three lots of precipitated formulation.

Given that the solid formulations from the three precipitations were very comparable, the three lots were blended into a single lot and subjected to further analytical characterization.

Potency analysis via an enzymatic assay showed that the precipitate was comparable to the mAb solution prior to precipitation with relative potencies of 96% and 103%, respectively. In addition, a large panel of biophysical assays was performed to elucidate any impact the precipitation process had on the quality attributes of mAb X.

Secondary (far UV CD), tertiary (near UV CD and Intrinsic Tryptophan Fluorescence), and higher-order structure analysis (DLS) showed that the precipitated mAb X was comparable to the reference standard representative of the mAb X process (Figure 3). Differential absorption of right- and left-handed circularly polarized light for the peptide in the range of 190–260 nm is a sensitive measure of its secondary structure. The far UV CD data (Figure 3A) showed comparable mean residual ellipticity for both precipitated mAb X and the reference standard representative of the mAb X.

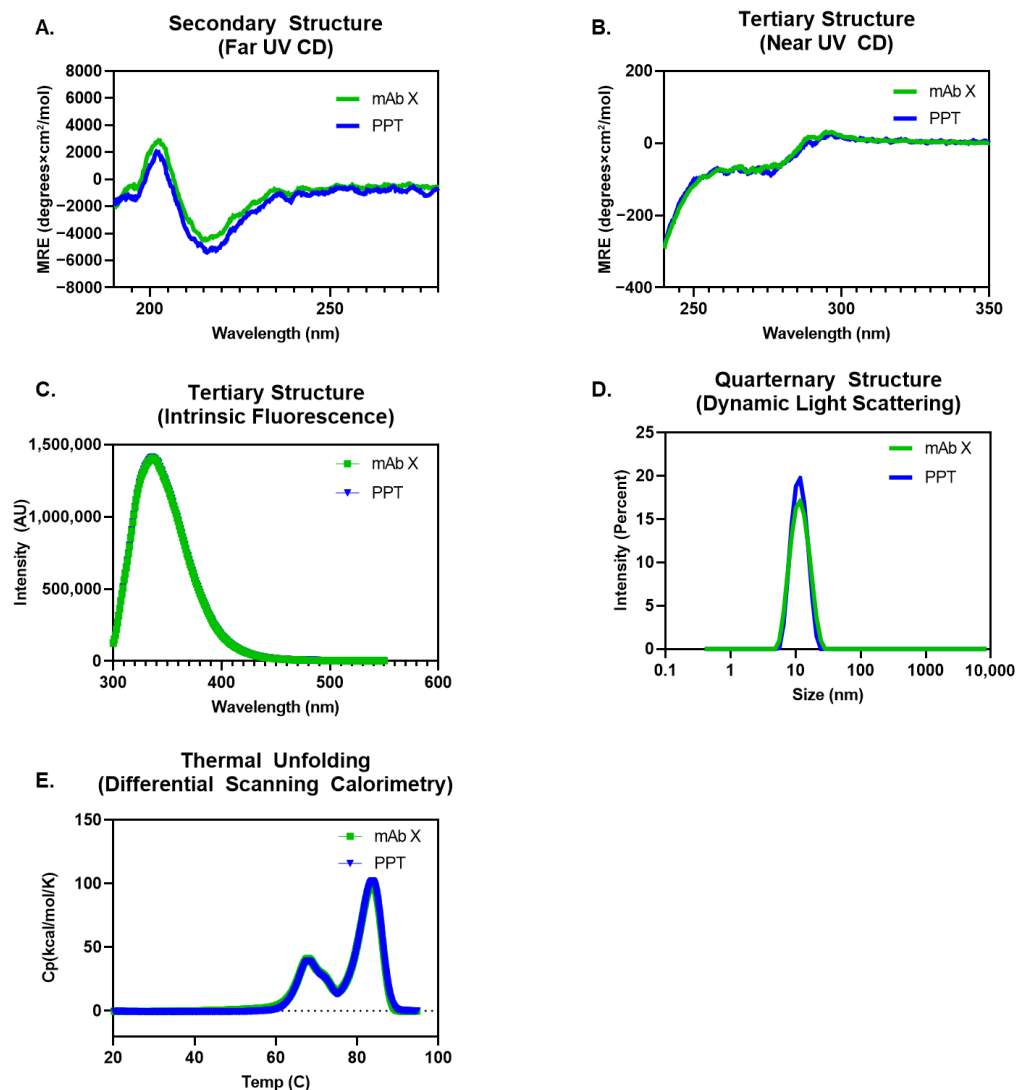


Figure 3. Comparison of secondary, tertiary, and higher-order structures of the reconstituted precipitated solid formulation (PPT) and mAb in solution (mAb X): (A) secondary structure via far UV CD; (B) tertiary structure via near UV CD; (C) tertiary structure via Intrinsic Tryptophan Fluorescence; and (D) higher-order structure via Dynamic Light Scattering. (E) The thermal stability of reconstituted precipitated solid formulation (PPT) and mAb in solution (mAb X) were determined using the DSC method. Changes in heat capacity (ΔC_p) were plotted against different temperatures.

Similarly, the differential absorbance of right- and left-handed circularly polarized light by aromatic amino acids (such as tryptophan, tyrosine, and phenylalanine) over the range of 240–320 nm can be used as a fingerprinting tool for tertiary structure analysis. A comparable level of differential absorbance was seen for right- and left-handed circularly polarized light over the range of 240–320 nm (Figure 3B) using near UV CD. These results were also validated by the intensity and position of the emission peak maxima for Intrinsic Tryptophan Fluorescence that show a comparable tertiary microenvironment (Figure 3C). The maximal fluorescence intensity (λ_{max}) was maintained at 337 nm, suggesting that the local environment of the aromatic amino acids may be partially solvent-exposed.

Dynamic Light Scattering (DLS) is used to report on the higher-order structure of the molecule. DLS measures the time-correlated fluctuation in local protein concentration in solution due to the Brownian motion of the molecules. Intensity-based size distribution (Figure 3D) showed a comparable particle size distribution between precipitated mAb X and the reference standard representative of the mAb X process.

For near UV CD, tryptophan peaks at 280–300 nm, tyrosine at 270–290 nm, and phenylalanine peaks between 250 and 270 nm are the fingerprints for tertiary structure. We see a clear overlay of spectra in these wavelength ranges, indicating similarity in tertiary structure. It is also validated by results from the Intrinsic Tryptophan Fluorescence, which shows clear overlap with no change in the lambda max (± 1 nm). If there were a process impact on the precipitated product and samples were not comparable, there would be a bigger shift in the lambda max. In this case, the lambda max does not change. Regarding Dynamic Light Scattering (DLS), the average peak size (Z average) and polydispersity index of these two samples are similar (within 1 nm variability). Typically, if the Z average is within 1 nm variability, the samples are deemed comparable. Differential Scanning Calorimetry (DSC) shows a similar unfolding trend between the two samples, indicating comparability. If precipitation had any impact in terms of structural rearrangement or formation of HMW species, we may see newer peaks during the unfolding process.

Differential Scanning Calorimetry (DSC) is used to assess the thermal unfolding behavior and here DSC thermograms showed a comparable thermal unfolding profile between precipitated mAb X and the reference standard representative of the mAb X process. Thermograms related to the change in the heat capacity against temperature changes are shown in Figure 3E.

Overall, analytical characterization demonstrated that the critical product attributes of mAb X were maintained during the precipitation process and very comparable to those of the pre-precipitation material. Moreover, extended characterization showed that the precipitated material has similar biological and biophysical properties.

3.2. Process Characterization

The impact of the precipitation parameters, i.e., temperature, mixing shear, and solvent/anti-solvent ratio on the quality attributes of the formulation was assessed using the experiments described in Table 1. Samples from each precipitation were analyzed and the high-level assessment is summarized in Figure 4. Samples 1, 1*, 2, 3, 4, and 5 were cloudy upon reconstitution and needed to be filtered. Samples 2 and 4 were particularly cloudy and required 1 mL of extra water to be added for full dissolution. Samples 5*, 6, and 7 were not cloudy and did not need to be filtered.

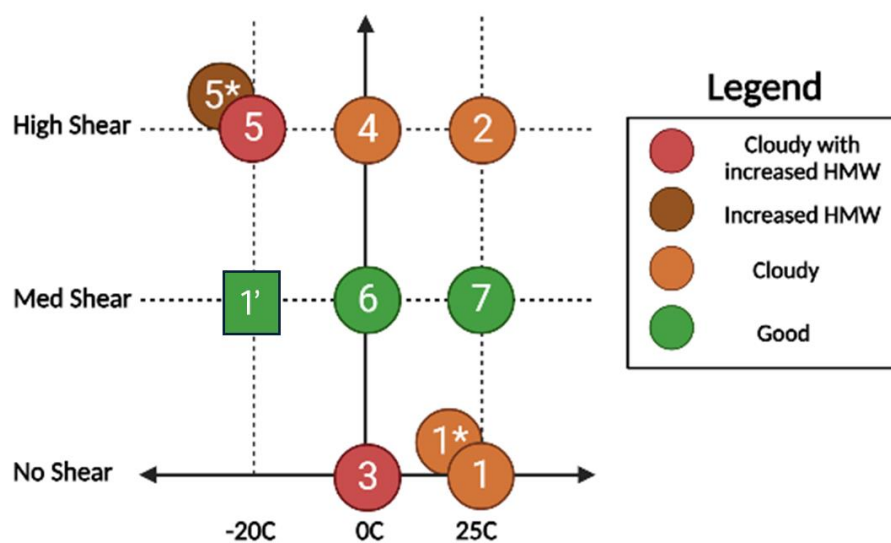


Figure 4. High-level assessment of the results of the precipitations in the process characterization experiments. * Corresponds to a different solvent-to-anti-solvent ration (3×); ' Corresponds to the initial triplicate run.

The samples from the precipitation were characterized using UP-SEC, HP-IEX, and CE-SDS, and the results are summarized in Table 2. The main “failure mode” is an increase in HMW %, which is indicative of aggregation. If we consider these results in conjunction with those of the initial triplicate precipitation (shown in Figure 4 as 1') carried out at medium shear and low solvent temperature, and which resulted in “good” characteristics upon precipitation, we can draw the conclusion that mixing shear is the primary factor affecting the quality attributes of the precipitated protein.

Table 2. Analytical characterization of the samples from the precipitation experiments.

Assay	Sample Number											
	mAb X	1'	1	1*	2	3	4	5	5*	6	7	
UP-SEC	Monomer %	99.1	98.6	98.2	99.0	99.6	96.8	98.9	97.9	94.2	99.3	99.4
	HMW species %	0.9	1.4	1.9	1.0	0.4	3.2	1.1	2.1	5.8	0.7	0.6
HP-IEX	Acidic variants %	15.8	18.6	16.5	17.5	18.1	17.6	18.1	18.3	16.9	18.0	17.9
	Total main %	51.9	51.5	53.6	52.7	52.7	51.3	52.0	51.3	51.8	52.5	52.6
	Basic variants %	32.3	29.9	29.9	29.8	29.3	31.1	29.9	30.4	31.3	29.6	29.5
Reduced CE-SDS	HC + LC %	97.9	98.6	99.3	99.3	99.3	99.3	99.3	99.3	99.2	99.3	99.3
	Total impurity %	2.1	1.4	0.7	0.7	0.7	0.7	0.7	0.7	0.8	0.7	0.7
Non-reduced CE-SDS	Intact IgG %	98.6	97.7	98.3	98.3	98.0	98.3	98.2	98.3	97.9	98.2	98.4
	Total LMW species %	1.4	2.2	1.6	1.6	1.9	1.5	1.7	1.5	1.9	1.8	1.5

* A different solvent to anti-solvent volume ratio was used (3×); 1' corresponds to the conditions of the initial triplicate run.

It can be hypothesized that there exists an optimal precipitation kinetic range where the protein precipitates at the same rate as the stabilizing sugars as well as an optimal shear environment. Slower mixing could potentially lead to a mismatch in the precipitation rate of the sugars and the protein, allowing for aggregation of the denatured proteins. On the other end of the spectrum, the high shear environment in the IKA ULTRA-TURRAX® could also lead to protein aggregation [54].

3.3. Stability of the Precipitated Formulations

In addition to assessing the potential impact of precipitation on the quality of the mAb X, further investigation was conducted to understand the stability performance of the precipitated material. Improvement in the stability of mAb X was critical for its development as it has been shown to have chemical instability under refrigerated conditions. In particular, the complementary determining region for mAb X is known to have the propensity to form succinimide intermediates, which have been shown to negatively impact the potency of mAb X [53]. The formation of the succinimide intermediate can be detected via ion exchange chromatography as an increase in the basic variants of mAb X.

The precipitated mAb X was staged in glass vials protected from light at 5 °C, 25 °C, and 40 °C and its chemical and physical stability was compared to that of the liquid formulation of mAb X. As shown in Figure 5, at 25 °C, the basic variants in the liquid formulation of mAb X grow appreciably, reflecting the formation of the succinimide intermediate. In contrast, the basic variants were stable in the precipitated formulation, showing minimal change at 25 °C after 3 months. With respect to the acidic variants, there was some growth observed in the precipitated material at 25 °C and under the refrigerated storage condition. With respect to physical stability, the liquid formulation and precipitated mAb X had similar stability as reflected in the HMW species, LMW species, and total impurities.

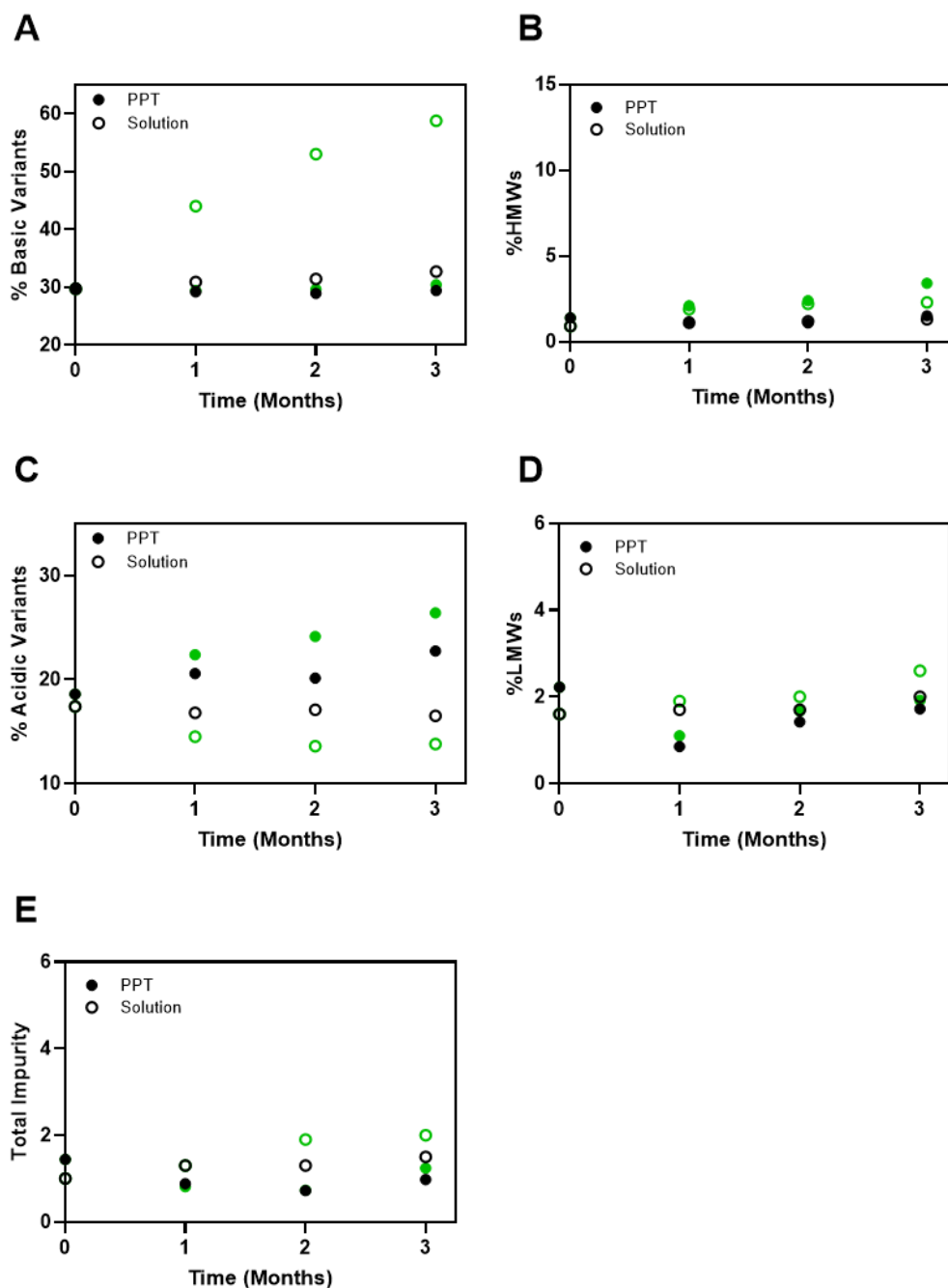


Figure 5. Comparison of % of basic variants (A), % of HMW species (B), % of acidic variants (C), % of LMW species (D), and % of total impurity (E) of precipitated mAb X (●) and mAb X in a solution formulation (○) stored at 5 °C (black) and 25 °C (green) for 3 months.

In addition, the stability profiles of the precipitation and lyophilized formulation of mAb X were compared. As shown in Figure 6A, the precipitated material was shown to have similar stability as the lyophilized formulation for up to 3 months at 40 °C with respect to slowing down succinimide formation. Similar to the comparison to the liquid formulation, the formation of acidic variants (Figure 6B) was accelerated in the precipitated material compared to the lyophilized formulation, which is likely due to an increase in deamidation and oxidation, suggested by mass spectrometry analysis. In contrast, the level of aggregation of the precipitated material was noticeably elevated at the 40 °C stressed condition compared to the lyophilized formulation (Figure 6C). In order to understand this phenomenon, an analysis of the process residuals was performed and the results showed

that the water content of the lyophilized cake and precipitated powder was 2.4 wt% and 4.2 wt%, respectively. In addition, residual solvent analysis of the precipitated material showed a significant level of residual acetone at 7.7 wt%. We hypothesize that the appreciable level of acetone in the precipitated material played a significant role in the formation of high molecular weight species on stability. Prior work has shown the potential of humid drying as a way to mitigate thermal exposure of sensitive materials and avoid form collapse that can trap solvents in amorphous materials. This should be evaluated for future studies to assess the capacity to achieve lower levels of residual solvent [55]. Lastly, the analysis of surfactant data showed that the surfactant in the formulation was not precipitated, which could be another factor contributing to the subpar stability performance of the precipitated mAb X. Additional process optimization will be conducted to address these concerns.

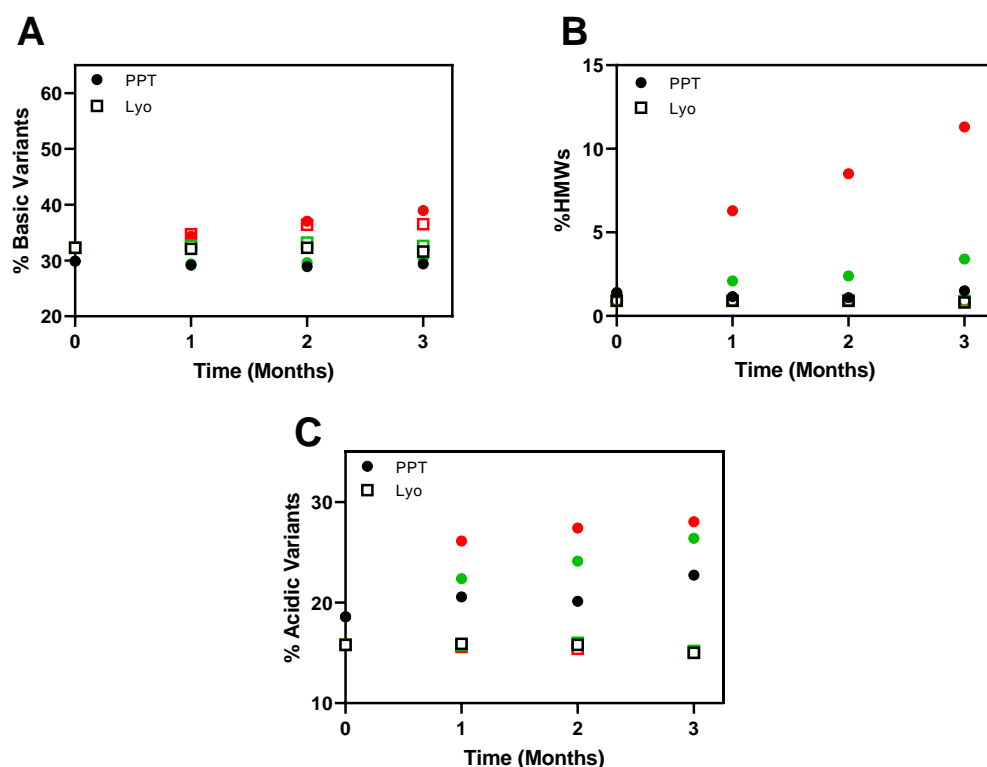


Figure 6. Comparison of % of basic variants (A), % of HMW species (B), and % of acidic variants (C) of precipitated mAb X (●) and mAb X in a lyophilized formulation (□) at 5 °C (black), 25 °C (green), and 40 °C (red) for 3 months.

4. Conclusions and Future Work

The co-precipitation of proteins and excipients into organic solvents has been shown to have the potential as a fast, cost-effective, and scalable process for the manufacture of solid formulations of therapeutic biologics. We have demonstrated that the process is robust and reproducible and, if carried out in a parameter range optimized to a specific molecule, results in isolated solids comparable to those obtained from lyophilization at time zero.

For stability during long-term storage, precipitated formulations provide a substantial improvement over the solution state. Comparisons with lyophilized formulations show the stability of the precipitated formulation being comparable with respect to certain degradation mechanisms and inferior in others. The latter is likely due to sub-optimal drying of the precipitated solids. Possible underlying mechanisms could involve the residual solvent promoting molecular mobility by suppressing the glass transition temperature of the solid and/or preferential interactions between the solvent and hydrophobic and aromatic residues on the mAb, causing changes in the higher-order structure.

Another potential factor influencing the stability of the precipitated formulation is that the surfactant in the mAb solution does not precipitate alongside the protein and other excipients, resulting in a substantial reduction in the stability of the reconstituted formulation.

Future work should include optimization of the drying process, perhaps implementing “humid” drying [55] to prevent structure collapse and solvent entrapment, as well as assessing different precipitation environments and/or different surfactants to ensure surfactant co-precipitation.

Author Contributions: Conceptualization, A.A.K., J.R.B., L.S. and D.F.; Formal analysis, W.L., B.P., Z.L., R.R. and Z.V.; Investigation, A.A.K., W.L. and N.H.; Data curation, B.P., Z.L., R.R., N.H. and Z.V.; Writing—original draft, A.A.K., W.L., J.R.B. and L.S.; Writing—review & editing, B.P., Z.L., R.R., D.F. and Z.V.; Visualization, B.P. All authors have read and agreed to the published version of the manuscript.

Funding: This research received no external funding.

Institutional Review Board Statement: Not applicable.

Informed Consent Statement: Not applicable.

Data Availability Statement: The original contributions presented in this study are included in the article. Further inquiries can be directed to the corresponding authors.

Acknowledgments: We gratefully acknowledge Timothy Toner for potency analysis, Jonathan Welch for surfactant measurement, Tuyen Cao for TGA-IR measurements, and Casey Dougherty-Gunsch for residual solvent and moisture measurements. The authors would also like to thank Ecevit Bilgili for contributing to discussions and providing suggestions regarding the publication of this research in the *Journal of Pharmaceutical and Biotech Industry*. Ecevit Bilgili was an amazing colleague, collaborator, and researcher—he will be missed!

Conflicts of Interest: All authors are the employees from Merck & Co., Inc.

References

1. Senior, M. Fresh from the biotech pipeline: Fewer approvals, but biologics gain share. *Nat. Biotechnol.* **2023**, *41*, 174–182. [[CrossRef](#)] [[PubMed](#)]
2. Chen, Y.; Mutukuri, T.T.; Wilson, N.E.; Zhou, Q. Pharmaceutical protein solids: Drying technology, solid-state characterization and stability. *Adv. Drug Deliv. Rev.* **2021**, *172*, 211–233. [[CrossRef](#)] [[PubMed](#)]
3. Sharma, A.; Khamar, D.; Cullen, S.; Hayden, A.; Hughes, H. Innovative Drying Technologies for Biopharmaceuticals. *Int. J. Pharm.* **2021**, *609*, 121115. [[CrossRef](#)] [[PubMed](#)]
4. Stratta, L.; Capozzi, L.C.; Franzino, S.; Pisano, R. Economic Analysis of a Freeze-Drying Cycle. *Processes* **2020**, *8*, 1399. [[CrossRef](#)]
5. Heller, M.C.; Carpenter, J.F.; Randolph, T.W. Protein formulation and lyophilization cycle design: Prevention of damage due to freeze-concentration induced phase separation. *Biotechnol. Bioeng.* **1999**, *63*, 166–174. [[CrossRef](#)]
6. Kasper, J.C.; Friess, W. The freezing step in lyophilization: Physico-chemical fundamentals, freezing methods and consequences on process performance and quality attributes of biopharmaceuticals. *Eur. J. Pharm. Biopharm.* **2011**, *78*, 248–263. [[CrossRef](#)]
7. Patel, S.M.; Nail, S.L.; Pikal, M.J.; Geidobler, R.; Winter, G.; Hawe, A.; Davagnino, J.; Rambhatla Gupta, S. Lyophilized Drug Product Cake Appearance: What Is Acceptable? *J. Pharm. Sci.* **2017**, *106*, 1706–1721. [[CrossRef](#)]
8. Jameel, F.; Alexeenko, A.; Bhambhani, A.; Sacha, G.; Zhu, T.; Tchessalov, S.; Sharma, P.; Moussa, E.; Iyer, L.; Luthra, S.; et al. Recommended Best Practices for Lyophilization Validation 2021 Part II: Process Qualification and Continued Process Verification. *AAPS PharmSciTech* **2021**, *22*, 266. [[CrossRef](#)]
9. Searles, J.; Ohtake, S. Strategies for Implementing New Drying & Packaging Technology for Sterile Injectable Drug Products. *J. Pharm. Sci.* **2021**, *110*, 1931–1934.
10. Ohtake, S.; Izutsu, K.; Lechuga-Ballesteros, D. *Drying Technologies for Biotechnology and Pharmaceutical Applications*; Wiley: New York, NY, USA, 2020.
11. Barcelo-Chong, C.M.; Filipe, V.; Nakach, M.; Inês Ré, M. How spray drying processing and solution composition can affect the mAbs stability in reconstituted solutions for subcutaneous injections. Part II: Exploring each protein stabilizer effect. *Int. J. Pharm.* **2024**, *655*, 124014. [[CrossRef](#)]

12. Pinto, J.T.; Faulhammer, E.; Dieplinger, J.; Dekner, M.; Makert, C.; Nieder, M.; Paudel, A. Progress in spray-drying of protein pharmaceuticals: Literature analysis of trends in formulation and process attributes. *Dry. Technol.* **2021**, *39*, 1415–1446. [[CrossRef](#)]
13. Tao, Y.; Chen, Y.; Howard, W.; Ibrahim, M.; Patel, S.M.; McMahon, W.P.; Kim, Y.J.; Delmar, J.A.; Davis, D. Mechanism of Insoluble Aggregate Formation in a Reconstituted Solution of Spray-Dried Protein Powder. *Pharm. Res.* **2023**, *40*, 2355–2370. [[CrossRef](#)] [[PubMed](#)]
14. Anandharamakrishnan, C.; Rielly, C.D.; Stapley, A.G.F. Loss of solubility of α -lactalbumin and β -lactoglobulin during the spray drying of whey proteins. *LWT—Food Sci. Technol.* **2008**, *41*, 270–277. [[CrossRef](#)]
15. Forbes, R.T.; Barry, B.W.; Elkordy, A.A. Preparation and characterisation of spray-dried and crystallised trypsin: FT-Raman study to detect protein denaturation after thermal stress. *Eur. J. Pharm. Sci.* **2007**, *30*, 315–323. [[CrossRef](#)]
16. Poozesh, S.; Mezhericher, M.; Pan, Z.; Chaudhary, U.; Manikwar, P.; Stone, H.A. Rapid Room-Temperature Aerosol Dehydration Versus Spray Drying: A Novel Paradigm in Biopharmaceutical Drying Technologies. *J. Pharm. Sci.* **2024**, *113*, 974–981. [[CrossRef](#)]
17. Adler, M.; Unger, M.; Lee, G. Surface Composition of Spray-Dried Particles of Bovine Serum Albumin/Trehalose/Surfactant. *Pharm. Res.* **2000**, *17*, 863–870. [[CrossRef](#)]
18. Hickey, A.J.; da Rocha, S.R. *Pharmaceutical Inhalation Aerosol Technology*; Hickey, A.J., da Rocha, S.R., Eds.; CRC Press: Boca Raton, FL, USA, 2019.
19. Abdul-Fattah, A.M.; Kalonia, D.S.; Pikal, M.J. The Challenge of Drying Method Selection for Protein Pharmaceuticals: Product Quality Implications. *J. Pharm. Sci.* **2007**, *96*, 1886–1916. [[CrossRef](#)]
20. Chang, R.Y.K.; Chow, M.Y.T.; Khanal, D.; Chen, D.; Chan, H.-K. Dry powder pharmaceutical biologics for inhalation therapy. *Adv. Drug Deliv. Rev.* **2021**, *172*, 64–79. [[CrossRef](#)]
21. Pan, H.W.; Seow, H.C.; Lo, J.C.K.; Guo, J.; Zhu, L.; Leung, S.W.S.; Zhang, C.; Lam, J.K.W. Spray-Dried and Spray-Freeze-Dried Powder Formulations of an Anti-Interleukin-4R α Antibody for Pulmonary Delivery. *Pharm. Res.* **2022**, *39*, 2291–2304. [[CrossRef](#)]
22. Bhambhani, A.; Stanbro, J.; Roth, D.; Sullivan, E.; Jones, M.; Evans, R.; Blue, J. Evaluation of Microwave Vacuum Drying as an Alternative to Freeze-Drying of Biologics and Vaccines: The Power of Simple Modeling to Identify a Mechanism for Faster Drying Times Achieved with Microwave. *AAPS PharmSciTech* **2021**, *22*, 52. [[CrossRef](#)]
23. Ambros, S.; Dombrowski, J.; Boettger, D.; Kulozik, U. The Concept of Microwave Foam Drying Under Vacuum: A Gentle Preservation Method for Sensitive Biological Material. *J. Food Sci.* **2019**, *84*, 1682–1691. [[CrossRef](#)] [[PubMed](#)]
24. Lovalenti, P.M.; Anderl, J.; Yee, L.; Nguyen, V.; Ghavami, B.; Ohtake, S.; Saxena, A.; Voss, T.; Truong-Le, V. Stabilization of Live Attenuated Influenza Vaccines by Freeze Drying, Spray Drying, and Foam Drying. *Pharm. Res.* **2016**, *33*, 1144–1160. [[CrossRef](#)] [[PubMed](#)]
25. Piетtre, M.; Vila, A. Sur la separation des proteines du serum. *Comptes Rendus Hebd. Seances Acad. Sci* **1920**, *170*, 1466–1468.
26. Barritault, D.; Expert-Bezançon, A.; Guérin, M.-F.; Hayes, D. The Use of Acetone Precipitation in the Isolation of Ribosomal Proteins. *Eur. J. Biochem.* **1976**, *63*, 131–135. [[CrossRef](#)]
27. Crowell, A.M.J.; Wall, M.J.; Doucette, A.A. Maximizing recovery of water-soluble proteins through acetone precipitation. *Anal. Chim. Acta* **2013**, *796*, 48–54. [[CrossRef](#)]
28. Jiang, L.; He, L.; Fountoulakis, M. Comparison of protein precipitation methods for sample preparation prior to proteomic analysis. *J. Chromatogr. A* **2004**, *1023*, 317–320. [[CrossRef](#)]
29. Aniket; Gaul, D.A.; Rickard, D.L.; Needham, D. MicroglassificationTM: A Novel Technique for Protein Dehydration. *J. Pharm. Sci.* **2014**, *103*, 810–820. [[CrossRef](#)]
30. Aniket; Gaul, D.A.; Bitterfield, D.L.; Su, J.T.; Li, V.M.; Singh, I.; Morton, J.; Needham, D. Enzyme Dehydration Using MicroglassificationTM Preserves the Protein's Structure and Function. *J. Pharm. Sci.* **2015**, *104*, 640–651. [[CrossRef](#)]
31. Chandrababu, K.B.; Kannan, A.; Savage, J.R.; Stadmler, S.; Ryle, A.E.; Cheung, C.; Kelley, R.F.; Maa, Y.-f.; Saggi, M.; Bitterfield, D.L. Stability Comparison Between Microglassification and Lyophilization Using a Monoclonal Antibody. *J. Pharm. Sci.* **2023**, *113*, 1054–1060. [[CrossRef](#)]
32. Yoshikawa, H.; Hirano, A.; Arakawa, T.; Shiraki, K. Mechanistic insights into protein precipitation by alcohol. *Int. J. Biol. Macromol.* **2012**, *50*, 865–871. [[CrossRef](#)]
33. Cohn, E.J.; Strong, L.E.; Hughes, W.L.J.; Mulford, D.J.; Ashworth, J.N.; Melin, M.E.; Taylor, H.L. Preparation and properties of serum and plasma proteins; a system for the separation into fractions of the protein and lipoprotein components of biological tissues and fluids. *J. Am. Chem. Soc.* **1946**, *68*, 459–475. [[CrossRef](#)] [[PubMed](#)]
34. Somasundaram, B.; Pleitt, K.; Shave, E.; Baker, K.; Lua, L.H.L. Progression of continuous downstream processing of monoclonal antibodies: Current trends and challenges. *Biotechnol. Bioeng.* **2018**, *115*, 2893–2907. [[CrossRef](#)] [[PubMed](#)]
35. Li, Z.; Chen, T.-H.; Andini, E.; Coffman, J.L.; Przybycien, T.; Zydney, A.L. Enhanced filtration performance using feed-and-bleed configuration for purification of antibody precipitates. *Biotechnol. Prog.* **2021**, *37*, e3082. [[CrossRef](#)] [[PubMed](#)]
36. Sommer, R.; Satzer, P.; Tscheliessnig, A.; Schulz, H.; Helk, B.; Jungbauer, A. Combined polyethylene glycol and CaCl₂ precipitation for the capture and purification of recombinant antibodies. *Process Biochem.* **2014**, *49*, 2001–2009. [[CrossRef](#)]

37. Li, Z.; Zydney, A.L. Effect of zinc chloride and PEG concentrations on the critical flux during tangential flow microfiltration of BSA precipitates. *Biotechnol. Prog.* **2017**, *33*, 1561–1567. [[CrossRef](#)]
38. Mullerpatan, A.; Chandra, D.; Kane, E.; Karande, P.; Cramer, S. Purification of proteins using peptide-ELP based affinity precipitation. *J. Biotechnol.* **2020**, *309*, 59–67. [[CrossRef](#)]
39. Swartz, A.R.; Xu, X.; Traylor, S.J.; Li, Z.J.; Chen, W. High-efficiency affinity precipitation of multiple industrial mAbs and Fc-fusion proteins from cell culture harvests using Z-ELP-E2 nanocages. *Biotechnol. Bioeng.* **2018**, *115*, 2039–2047. [[CrossRef](#)]
40. Kateja, N.; Agarwal, H.; Saraswat, A.; Bhat, M.; Rathore, A.S. Continuous precipitation of process related impurities from clarified cell culture supernatant using a novel coiled flow inversion reactor (CFIR). *Biotechnol. J.* **2016**, *11*, 1320–1331. [[CrossRef](#)]
41. Sommer, R.; Tscheliessnig, A.; Satzer, P.; Schulz, H.; Helk, B.; Jungbauer, A. Capture and intermediate purification of recombinant antibodies with combined precipitation methods. *Biochem. Eng. J.* **2015**, *93*, 200–211. [[CrossRef](#)]
42. Brodsky, Y.; Zhang, C.; Yigzaw, Y.; Vedantham, G. Caprylic acid precipitation method for impurity reduction: An alternative to conventional chromatography for monoclonal antibody purification. *Biotechnol. Bioeng.* **2012**, *109*, 2589–2598. [[CrossRef](#)]
43. Ma, J.; Hoang, H.; Myint, T.; Peram, T.; Fahrner, R.; Chou, J.H. Using precipitation by polyamines as an alternative to chromatographic separation in antibody purification processes. *J. Chromatogr. B* **2010**, *878*, 798–806. [[CrossRef](#)] [[PubMed](#)]
44. Kang, Y.; Hamzik, J.; Felo, M.; Qi, B.; Lee, J.; Ng, S.; Liebisch, G.; Shanehsaz, B.; Singh, N.; Persaud, K.; et al. Development of a novel and efficient cell culture flocculation process using a stimulus responsive polymer to streamline antibody purification processes. *Biotechnol. Bioeng.* **2013**, *110*, 2928–2937. [[CrossRef](#)] [[PubMed](#)]
45. Singh, N.; Arunkumar, A.; Chollangi, S.; Tan, Z.G.; Borys, M.; Li, Z.J. Clarification technologies for monoclonal antibody manufacturing processes: Current state and future perspectives. *Biotechnol. Bioeng.* **2016**, *113*, 698–716. [[CrossRef](#)] [[PubMed](#)]
46. McNerney, T.; Thomas, A.; Senczuk, A.; Petty, K.; Zhao, X.; Piper, R.; Carvalho, J.; Hammond, M.; Sawant, S.; Bussiere, J. PDADMAC flocculation of Chinese hamster ovary cells: Enabling a centrifuge-less harvest process for monoclonal antibodies. *mAbs* **2015**, *7*, 413–427. [[CrossRef](#)] [[PubMed](#)]
47. Li, Z.; Chen, J.; Martinez-Fonts, K.; Rauscher, M.; Rivera, S.; Welsh, J.; Kandula, S. Cationic polymer precipitation for enhanced impurity removal in downstream processing. *Biotechnol. Bioeng.* **2023**, *120*, 1902–1913. [[CrossRef](#)]
48. Chang, L.; Pikal, M.J. Mechanisms of protein stabilization in the solid state. *J. Pharm. Sci.* **2009**, *98*, 2886–2908. [[CrossRef](#)]
49. Mensink, M.A.; Frijlink, H.W.; van der Voort Maarschalk, K.; Hinrichs, W.L.J. How sugars protect proteins in the solid state and during drying (review): Mechanisms of stabilization in relation to stress conditions. *Eur. J. Pharm. Biopharm.* **2017**, *114*, 288–295. [[CrossRef](#)]
50. Carpenter, J.F.; Crowe, J.H. An infrared spectroscopic study of the interactions of carbohydrates with dried proteins. *Biochemistry* **1989**, *28*, 3916–3922. [[CrossRef](#)]
51. Prestrelski, S.J.; Tedeschi, N.; Arakawa, T.; Carpenter, J.F. Dehydration-induced conformational transitions in proteins and their inhibition by stabilizers. *Biophys. J.* **1993**, *65*, 661–671. [[CrossRef](#)]
52. Arsiccio, A.; Pisano, R. Water entrapment and structure ordering as protection mechanisms for protein structural preservation. *J. Chem. Phys.* **2018**, *148*, 055102. [[CrossRef](#)]
53. VanAernum, Z.L.; Sergi, J.A.; Dey, M.; Toner, T.; Kilgore, B.; Lay-Fortenbery, A.; Wang, Y.; Bian, S.; Kochert, B.A.; Bothe, J.R.; et al. Discovery and Control of Succinimide Formation and Accumulation at Aspartic Acid Residues in The Complementarity-Determining Region of a Therapeutic Monoclonal Antibody. *Pharm. Res.* **2023**, *40*, 1411–1423. [[CrossRef](#)] [[PubMed](#)]
54. Wang, W.; Nema, S.; Teagarden, D. Protein aggregation—Pathways and influencing factors. *Int. J. Pharm.* **2010**, *390*, 89–99. [[CrossRef](#)] [[PubMed](#)]
55. Lamberto, D.J.; Diaz-Santana, A.; Zhou, G. Form Conversion and Solvent Entrapment during API Drying. *Org. Process Res. Dev.* **2017**, *21*, 1828–1834. [[CrossRef](#)]

Disclaimer/Publisher’s Note: The statements, opinions and data contained in all publications are solely those of the individual author(s) and contributor(s) and not of MDPI and/or the editor(s). MDPI and/or the editor(s) disclaim responsibility for any injury to people or property resulting from any ideas, methods, instructions or products referred to in the content.